J. Mater. Environ. Sci. 4 (5) (2013) 583-592
ISSN : 2528-2028
CODEN: JMESCN

Studies on the Inhibitive Effect of the Ammonium Iron (II) Sulphate on the Corrosion of Carbon Steel in HCl Solution

A. Anejjar[1], A. Zarrouk[2], R. Salghi[1,*], H. Zarrok[3], D. Ben Hmamou[1], B. Hammouti[2], B. Elmahi[2], S.S. Al-Deyab[5]

[1]*Laboratory of Environmental Engineering and Biotechnology, ENSA, University Ibn Zohr, 80000 Agadir, Morocco*
[2]*LCAE-URAC 18, Faculty of Science, University of Mohammed Premier, Po Box 717 60000 Oujda, Morocco*
[3]*Laboratory separation processes, Faculty of Science, University Ibn Tofail PO Box 242, Kenitra, Morocco.*
[4]*Petrochemical Research Chair, Chemistry Department, College of Science, King Saud University, P.O. Box 2455, Riyadh 11451, Saudi Arabia.*

Received 10 Jan 2013; Revised 6 Apr 2013, Accepted 6 Apr 2013
*Corresponding Author. R. Salghi, e-mail: r_salghi@yahoo.fr

Abstract
Electrochemical impedance spectroscopy (EIS), potentiodynamic polarization and gravimetric, techniques were carried out to investigate the corrosion protection properties of ammonium iron (II) sulphate (AIS) on carbon steel in 1 M HCl solution. The EIS study indicated that the addition of AIS in corrosive medium increases the charge-transfer resistance (R_{ct}), decreases the double-layer capacitance (C_{dl}) of the corrosion process, and hence increases the inhibition performance. Potentiodynamic polarization measurements showed that the presence of AIS in 1 M HCl solutions decreased corrosion currents to a great extent. The above results showed that AIS acted as a mixed-type corrosion inhibitor. Moreover, the thermodynamic activation parameters for the corrosion reaction were calculated and discussed in relation to the stability of the protective inhibitor layer. Adsorption of inhibitor was found to obey Langmuir isotherm. The thermodynamic parameter value of free energy of adsorption (ΔG^{o}_{ads}) reveals that inhibitor was adsorbed on the carbon steel surface via both physisorption and chemisorption mechanism.

Keywords: Inorganic inhibitor, Carbon steel, HCl, Adsorption.

1. Introduction
Corrosion is a fundamental process playing an important role in economics and safety, particularly for metals and alloys. Steel has found wide application in a broad spectrum of industries and machinery; however its tendency to corrosion. The corrosion of steel is a fundamental academic and industrial concern that has received a considerable amount of attention. Among several methods used in combating corrosion problems, the use of chemical inhibitors remains the most cost effective and practical method. Therefore, the development of corrosion inhibitors based on organic compounds containing nitrogen, sulphur and oxygen atoms are of growing interest in the field of corrosion and industrial chemistry as corrosion poses serious problem to the service lifetime of alloys used in industry [1-17]. Little work [18-21] appears to have been done on the inhibition of steel in HCl solution by inorganic compounds. The purpose of this paper is to evaluate the corrosion of carbon steel in the absence and the presence of Ammonium Iron (II) Sulphate (AIS) in 1 M HCl. The inhibition effect of AIS on carbon steel in 1 M HCl is studied for the first time by electrochemical impedance spectroscopy (EIS), potentiodynamic polarisation curves and weight loss methods. The adsorption isotherm of AIS on carbon steel surface is discussed in detail at the range of inhibitor concentrations. The adsorption free energy ΔG^{o}_{ads} was also calculated and correlated to the adsorption process.

2. Experimental
Materials
The tested inhibitor, namely, Ammonium Iron (II) Sulphate ($(NH_4)_2Fe(SO_4)_2.6H_2O$) (AIS) was obtained from Sigma–Aldrich chemical co. and his chemical structure is presented in Fig. 1. The steel used in this

ISSN : 2528-2028
CODEN: JMESCN

study is a carbon steel (CS) (Euronorm: C35E carbon steel and US specification: SAE 1035) with a chemical composition (in wt%) of 0.370 % C, 0.230 % Si, 0.680 % Mn, 0.016 % S, 0.077 % Cr, 0.011 % Ti, 0.059 % Ni, 0.009 % Co, 0.160 % Cu and the remainder iron (Fe). The aggressive solutions of 1 M HCl were prepared by dilution of analytical grade 37% HCl with distilled water. The concentration range of AIS empl was 10^{-2} to 10^{-5} M.

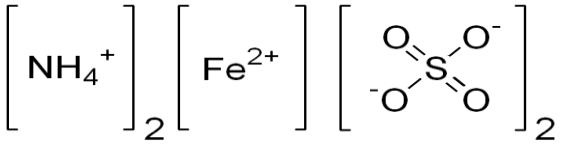

Fig.1: Structure of Ammonium Iron (II) Sulphate molecule (AIS).

Electrochemical measurements

Electrochemical impedance spectroscopy

The electrochemical measurements were carried out using Volta lab (Tacussel- Radiometer PGZ 100) potentiostate and controlled by Tacussel corrosion analysis software model (Voltamaster 4) at under static condition. The corrosion cell used had three electrodes. The reference electrode was a saturated calomel electrode (SCE). A platinum electrode was used as auxiliary electrode of surface area of 0.094 cm^2. The working electrode was carbon steel. All potentials given in this study were referred to this reference electrode. The working electrode was immersed in test solution for 30 minutes to a establish steady state open circuit potential (E_{ocp}). After measuring the E_{ocp}, the electrochemical measurements were performed. All electrochemical tests have been performed in aerated solutions at 298 K. The EIS experiments were conducted in the frequency range with high limit of 100 kHz and different low limit 0.1 Hz at open circuit potential, with 10 points per decade, at the rest potential, after 30 min of acid immersion, by applying 10 mV ac voltage peak-to-peak. Nyquist plots were made from these experiments. The best semicircle can be fit through the data points in the Nyquist plot using a non-linear least square fit so as to give the intersections with the *x*-axis. In this case, the inhibition efficiency $\eta_Z(\%)$ is calculated by R_{ct} using the following equation:

$$\eta_Z(\%) = \frac{1/R_{ct}^0 - 1/R_{ct}}{1/R_{ct}^0} \times 100 \quad (1)$$

where R_{ct}^0 and R_{ct} are the charge-transfer resistance values without and with inhibitor [22], respectively.

Potentiodynamic polarization

The electrochemical behavior of carbon steel sample in inhibited and uninhibited solution was studied by recording anodic and cathodic potentiodynamic polarization curves. Measurements were performed in the 1 M HCl solution containing different concentrations of the tested inhibitor by changing the electrode potential automatically from -800 to -400 mV versus corrosion potential at a scan rate of 1 mV s^{-1}.

Weight loss measurements

Coupons were cut into 2 × 2 × 0.08 cm^3 dimensions are used for weight loss measurements. Prior to all measurements, the exposed area was mechanically abraded with 180, 320, 800, 1200 grades of emery papers. The specimens were washed thoroughly with bidistilled water, degreased and dried with ethanol. Gravimetric measurements are carried out in a double walled glass cell equipped with a thermostated cooling condenser. The solution volume is 80 mL. The immersion time for the weight loss is 6 h at 298 K.

3. Results and Discussion

Polarization curves

Fig. 2 shows the potentiodynamic polarization curves after the addition of AIS. In every curve, it is observed that the current densities of the anodic and cathodic branch are displaced towards lower values. This displacement is more evident with the increase in concentration of the corrosion inhibitor when compared to the uninhibited solution. Electrochemical kinetic parameters (corrosion potential (E_{corr}), corrosion current density (I_{orr}) and cathodic Tafel slope (β_c)), determined from the polarisation curves by Tafel extrapolation method, are reported in Table 1. Table 1 also included percentage inhibition efficiency, η_{Tafel} (%), that was calculated from the following equation [23,24]:

ISSN : 2528-2028
CODEN: JMESCN

$$E(\%) = \frac{I^{o}_{corr} - I_{corr}}{I^{o}_{corr}} \times 100 \quad (2)$$

where I^{o}_{corr} and I_{corr} are the corrosion current densities for steel electrode in the uninhibited and inhibited solutions, respectively.

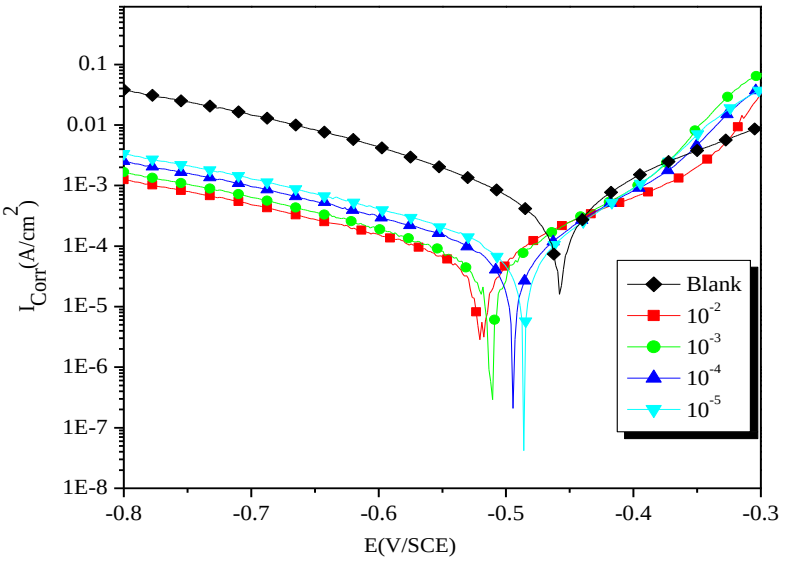

Figure 2. Potentiodynamic polarisation curves of carbon steel in 1 M HCl in the presence of different concentrations of AIS.

From Table 1, the corrosion current density decreased with the increase of the inhibitor concentration and η_{Tafel} % showed the opposite trend which indicated that the inhibitor suppressed the carbon steel corrosion in 1 M HCl solution. The presence of AIS resulted in no definite trend in the shift of E_{corr} compared to that in the absence of AIS, however, the displacement in E_{corr} is < 85 mV. These results indicated that the presence of AIS inhibited both iron oxidation and hydrogen evolution, consequently AIS can be classified as mixed corrosion inhibitor [25-27] with the inhibitory action caused by a geometric blocking effect [28]. In addition, the inhibitory action was due to a reduction of the reaction area on the surface of the corroding metal [29].

Table 2. Electrochemical parameters of carbon steel at various concentrations of AIS in 1 M HCl and corresponding inhibition efficiency.

	Concentration (M)	E_{corr} (mV/SCE)	I_{corr} (µA/cm^2)	$-\beta_c$ (mV/dec)	η_{Tafel} (%)
Blank	----	-457	594	190	----
	10^{-2}	-518	82	188	86.2
AIS	10^{-3}	-510	95	186	84.0
	10^{-4}	-494	105	175	82.3
	10^{-5}	-486	136	156	77.1

Electrochemical impedance spectroscopy measurements

The impedance spectra for carbon steel in 1 M HCl solution without and with various concentrations of AIS are presented as Nyquist plots in Fig. 3. From these plots, the impedance response of mild steel has significantly changed on addition of the AIS. For analysis of the impedance spectra containing a depressed capacitive semi circle [30], the standard Randle circuit is shown in Fig.4 [31,32]. The depression in Nyquist semicircles is a feature for solid electrodes and often referred to as frequency dispersion and attributed to the roughness and other inhomogenities of the solid electrode [33,34]. C_{dl} is replaced by a constant phase element (CPE) with the exponent, *n*. It is found that the Nyquist plots for various concentrations of AIS inhibitor showed similar trend of curves which was depressed semicircle with the centre located below the real x-axis. Increasing the inhibitor concentration will increase the size of the curves, indicating the time constant of the charge transfer and double-layer capacitance [35]. This behavior shows the adsorption of AIS on carbon steel surface.

ISSN : 2528-2028
CODEN: JMESCN

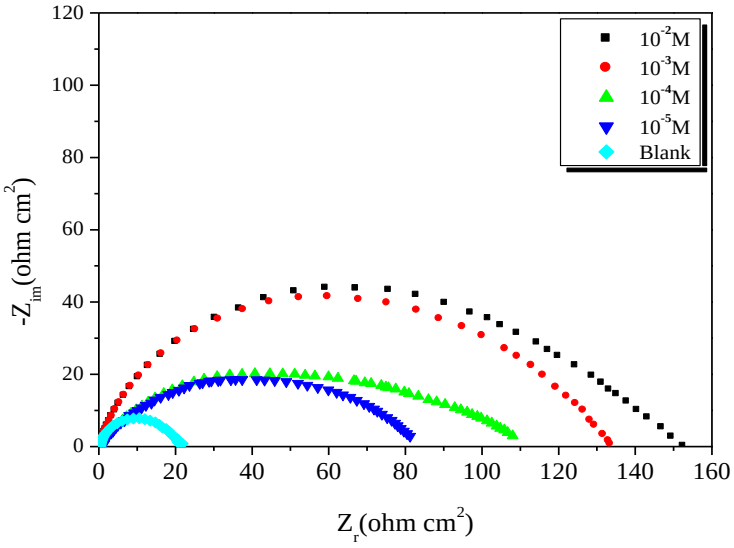

Figure 3. Nyquist diagrams for carbon steel electrode with and without AIS at E_{corr} after 30 min of immersion.

It is also found that from the Nyquist plots, even with the addition or absence of inhibitor does not alter the style of impedance curves, thus proposing a similar mechanism of inhibition is involved. The impedance parameters derived from these plots are given in Table 2. As noted from Table 2, the polarization resistances values containing inhibitor substantially increased along the concentration compared to that without inhibitor. It is also clear that the value of C_{dl} decreases on the addition of inhibitor, indicating a decrease in the local dielectric constant and/or an increase in the thickness of the electrical double layer, suggesting the inhibitor molecules function by the formation of the protective layer at the metal surface.

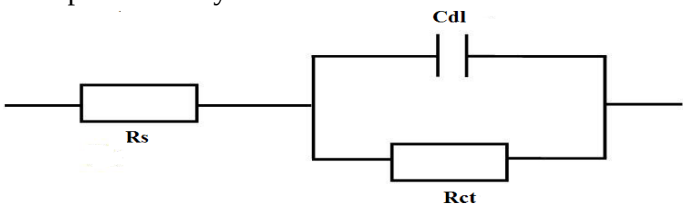

Figure 4. The standard Randle circuit.

Table 2. Electrochemical Impedance parameters for corrosion of carbon steel in acid medium at various contents concentrations of AIS.

Inhibitor	Conc (M)	R_{ct} (Ω cm^2)	C_{dl} (μF cm^{-2})	η_Z (%)
Blank	----	21	85.31	----
AIS	10^{-2}	153	16.01	86.3
	10^{-3}	134	26.02	84.3
	10^{-4}	111	29.71	81.1
	10^{-5}	82	36.10	74.4

Weight loss measurements
Effect of concentration

Weight loss experiments were done according to the method described previously [17]. Weight loss measurements were performed at 298 K for 6 h by immersing the carbon steel coupons into acid solution (80 mL) without and with various amounts of inhibitor. After the elapsed time, the specimen were taken out, washed, dried and weighed accurately. The inhibition efficiency (μ_{WL}%) and surface coverage (θ) was determined by using following equations:

ISSN : 2528-2028
CODEN: JMESCN

$$\mu_{WL}\% = \frac{w_0 - w_i}{w_0} \times 100 \quad (3)$$

$$\theta = \frac{w_0 - w_i}{w_0} \quad (4)$$

where, w_0 and w_i are the weight loss value in the absence and presence of inhibitor.
Initially carbon steel corroded at higher rate in acid but presence of inhibitor retarded the corrosion rate and remarkable improvement in inhibition efficiency was achieved (Figure 5). It was observed from Figure 5 that corrosion rate was decreasing with increasing inhibitor concentration whereas inhibition efficiency was increased with increasing amount of inhibitor. Maximum inhibition efficiency of 85 % was found at 10^{-2} M inhibitor concentration. From data listed in Table 3 decreased value of weight loss was noticed with increasing concentration of inhibitor due to increased surface coverage which can be accounted for inhibitive action of inhibitor.

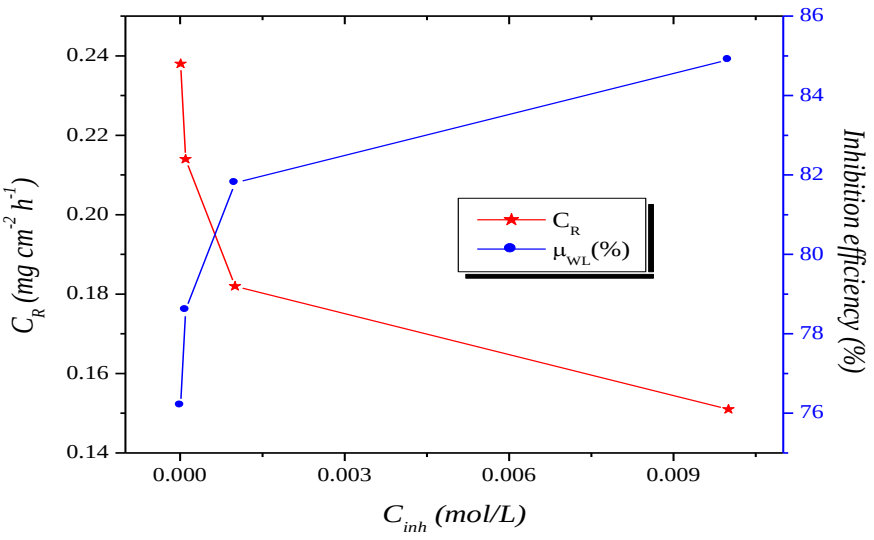

Figure 5. Corrosion rates and inhibition efficiencies obtained at different concentrations of inhibitor in 1 M HCl at 298K for 6h.

Table 3: Effect of AIS concentration on corrosion data of carbon steel in 1 M HCl.

Inhibitor	Concentration (M)	C_R (mg cm^{-2} h^{-1})	μ_{WL} (%)	θ
Blank	----	1.001	----	----
	10^{-2}	0.151	84.9	0.849
AIS	10^{-3}	0.182	81.8	0.818
	10^{-4}	0.214	78.6	0.786
	10^{-5}	0.238	76.2	0.762

Adsorption isotherm and thermodynamic
The action of an inhibitor in aggressive acid media is assumed to be due to its adsorption at the metal/solution interface. The adsorption process depends on the electronic characteristics of the inhibitor, the nature of metal surface, temperature, steric effects and the varying degrees of surface-site activity [36,37]. In fact, the solvent H_2O molecules could also be adsorbed at the metal/solution interface. Therefore, the adsorption of organic inhibitor molecules from the aqueous solution can be considered as a quasi substitution process between the organic compounds in the aqueous phase $Org_{(sol)}$ and water molecules at the electrode surface $H_2O_{(ads)}$ [38]:

$$Org_{(sol)} + xH_2O_{(ads)} \leftrightarrow xH_2O_{(sol)} + Org_{(ads)} \quad (6)$$

where x is the size ratio, that is, the number of water molecules replaced by one organic inhibitor. The type of the adsorption isotherm can provide additional information about the properties of the tested compounds. In

ISSN : 2528-2028
CODEN: JMESCN

order to obtain the adsorption isotherm, the degree of surface coverage (θ) of the inhibitor must be calculated. In this study, the degree of surface coverage values (θ) for various concentrations of the inhibitor in acidic media have been evaluated from the weight loss measurements and listed in Table 4. Attempts were made to fit the θ values to various isotherms, including Langmuir, Temkin, Frumkin and Flory-Huggins. By far, the best fit is obtained with the Langmuir isotherm. Langmuir adsorption isotherm is described by the following equations:

$$\frac{\theta}{1-\theta} = K_{ads} C_{inh} \qquad (7)$$

By rearranging this equation:

$$\frac{C_{\text{inh}}}{\theta} = \frac{1}{K_{\text{ads}}} + C_{\text{inh}} \qquad (8)$$

where C_{inh} is the inhibitor concentration, K_{ads} is the adsorption equilibrium constant and θ is the surface coverage. Fig. 6 shows the plots of Cinh/θ versus C_{inh} and the expected linear relationship is obtained for AIS.

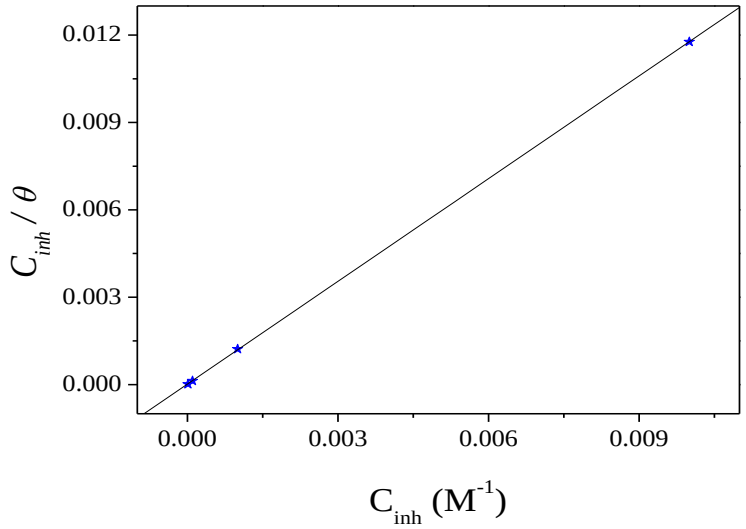

Figure 6. Langmuir adsorption of AIS on the carbon steel surface in 1.0 HCl solution.

The strong correlations (R^2 = 0.9995) confirm the validity of this approach. The slope of the straight line (K_{ads}) has been found to be 5.44×10^4 M^{-1} (Table 4) suggesting that the adsorbed inhibitor molecules form monolayer on the carbon steel surface and there is no interaction among the adsorbed inhibitor molecules [39]. On the other hand, the relatively high value of adsorption equilibrium constant reflects the high adsorption ability of AIS on carbon steel surface [40,41]. The standard free energy of adsorption (ΔG°_{ads}) can be given as the following equation:

$$\Delta G^{\circ}_{ads} = -RTLn(55.5K_{ads}) \qquad (9)$$

where R is the gas constant (8.314 J K^{-1} mol^{-1}), T is the absolute temperature (K), the value 55.5 is the concentration of water in solution expressed in M [42].

Table 4. Thermodynamic parameters for the adsorption of AIS in 1 M HCl on the carbon steel at 298K.

Inhibitor	Slope	K_{ads} (M^{-1})	R^2	ΔG°_{ads} (kJ/mol)
AIS	1.1	5.44×10^4	0.99	-36.95

The ΔG°_{ads} value is calculated as -36.95 kJ mol^{-1}. Generally, the values of ΔG°_{ads} up to -20 kJ mol^{-1} are consistent with the electrostatic interaction between the charged molecules and the charged metal (physical adsorption) while those more negative than 40 kJ mol^{-1} involve sharing or transfer of electrons from the inhibitor molecules to the metal surface to form a co-ordinate type of bond (chemisorption) [43,44]. In this

ISSN : 2528-2028
CODEN: JMESCN

study, the value of ΔG°_{ads} is slightly negative than -20 kJ mol^{-1}; which suggests that the adsorption mechanism of the AIS on steel in 1 M HCl solution is mainly the physical adsorption [45-47]. However, adsorption of inhibitor molecules is not merely physisorption or chemisorption, and it includes a comprehensive adsorption (physical and chemical adsorption) for the same values [48].

Effet of temperature

The effect of temperature on the inhibition efficiencies of AIS was also studied by EIS in the temperature range 298-328K (Figs. 7 and 8). From Figs. 7 and 8, and Table 5, it can be concluded that the R_{ct} values decreases in both uninhibited and inhibited solutions and the value of inhibition efficiency decreases slightly with the increase in the temperature. Thus AIS acts as a temperature-dependent inhibitor, and the relationship between temperature and inhibition efficiency is also a characteristic of the physical adsorption [49].

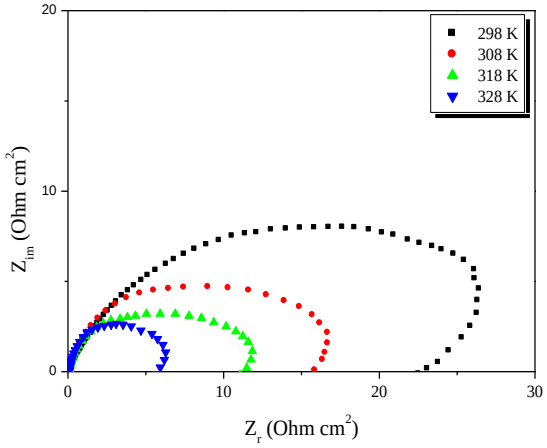

Figure 7. Nyquist diagrams for carbon steel in 1 M HCl at different temperatures.

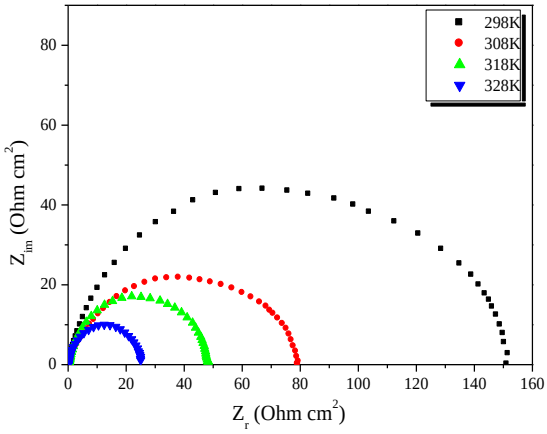

Figure 8. Nyquist diagrams for carbon steel in 1 M HCl + 10^{-2} mol/L of AIS at different temperatures.

Table 5. Effect of temperature on the carbon steel in free acid and at 10^{-2} M of AIS.

Inhibitor	T (K)	R_{ct} (Ω cm^2)	η_z (%)
Blank	298	21	----
	308	13	----
	318	10	----
	328	5.4	----
AIS	298	153	86.3
	308	80	83.7
	318	48	79.2
	328	25	78.4

Values of R_{ct} were employed to calculate values of the corrosion current density (I_{corr}) at various temperatures in absence and presence of AIS using the following equation [50]:

$$I_{corr} = RT\left(zFR_{ct}\right)^{-1} \quad (10)$$

where R is the universal gas constant (R = 8.314 J mol^{-1} K^{-1}), T is the absolute temperature, z is the valence of iron (z = 2), F is the Faraday constant (F = 96 485 coulomb) and R_{ct} is the charge transfer resistance.
Activation energy can be obtained by Arrhenius equation as follows

$$I_{corr} = k\exp\left(-\frac{E_a}{RT}\right) \quad (11)$$

ISSN : 2528-2028
CODEN: JMESCN

where E_a is the apparent activation corrosion energy, R is the universal gas constant and k is the Arrhenius pre-exponential constant. Taking the logarithm of the Arrhenius equation yields:

$$LnI_{corr} = \frac{-E_a}{RT} + Lnk \qquad (12)$$

EIS measurements were utilized to obtain the I_{corr} values using the equation (10) of carbon steel in the absence and presence of 10^{-2} M of AIS at different temperatures of 298, 308, 318 and 328K. These values were plotted as shown in Fig. 9. The values of activation energy of corrosion were determined from the slope of Ln (I_{corr}) versus 1/T plots [51]. The E_a values for carbon steel in the absence and presence of 10^{-2} M of AIS were calculated and listed in Table 6. The value of E_a found for AIS is higher than that obtained for 1 M HCl solution. The increase in the apparent activation energy may be interpreted as physical adsorption that occurs in the first stage [52]. Szauer and Brand explained that the increase in activation energy can be attributed to an appreciable decrease in the adsorption of the inhibitor on the carbon steel surface with increase in temperature.
A transition state complex is decays to products after forming the high energy [53]. The mathematical form of transition state theory is shown as below:

$$I_{corr} = \frac{RT}{Nh}\exp\left(\frac{\Delta S_a}{R}\right)\exp\left(-\frac{\Delta H_a}{RT}\right) \qquad (10)$$

where I_{corr} is the corrosion rate, A is the pre-exponential factor, h is Planck's constant, N is the Avogadro number, R is the universal gas constant, ΔH_a is the enthalpy of activation and ΔS_a is the entropy of activation.
The values of enthalpy and entropy of activation for carbon steel corrosion in 1 M HCl in absence and presence of AIS can be evaluated from the slope and intercept of the curve of Ln (I_{corr}/T) versus 1/T, respectively as shown in Fig. 10.

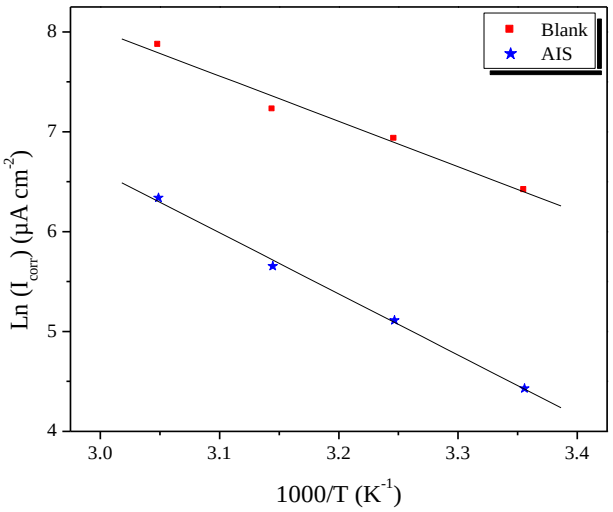

Figure 9. Arrhenius plots of carbon steel in 1 M HCl with and without 10^{-2} M of AIS.

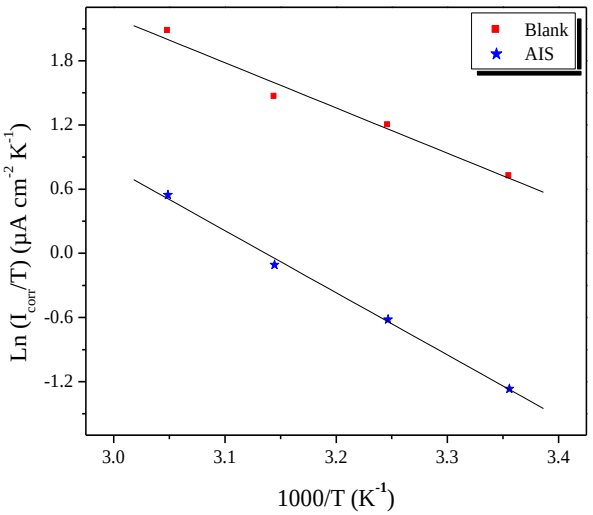

Figure 10. Relation between Ln (I_{corr}/ T) and 1000/T at different temperatures.

Table 6. The value of activation parameters for carbon steel in 1 M HCl in the absence and presence of 10^{-2} M of AIS.

Inhibitor	E_a (kJ/mol)	ΔH_a (kJ/mol)	ΔS_a (J/mol)	E_a -ΔH_a (KJ/mol)
Blank	37.75	35.15	-73.75	2.6
AIS	50.88	48.28	46.09	2.6

Inspection of these data revealed that the thermodynamic parameters (ΔS_a and ΔH_a) for dissolution reaction of carbon steel in 1 M HCl in the presence of inhibitor are higher than that obtained in the absence of inhibitor. The positive sign of ΔH_a reflects the endothermic nature of the carbon steel dissolution process suggesting that the dissolution of carbon steel is slow [54] in the presence of inhibitor. The large negative value of ΔS_a for carbon

steel in 1 M HCl implies that the activated complex is the rate-determining step, rather than the dissociation step. In the presence of the inhibitor, the value of ΔS_a increases and is generally interpreted as an increase in disorder as the reactants are converted to the activated complexes [45].

Conclusions

The inhibition effect of AIS on carbon steel in hydrochloric acid was examined by weight loss methods, potentiodynamic polarization and electrochemical impedance spectroscopy techniques. AIS act as a good corrosion inhibitor in 1 M HCl solutions. Inhibition efficiency value increases with the increasing of the inhibitor concentration, while the efficiency decreased with increasing the temperature. Polarization curves indicated that this inhibitor acts as mixed type inhibitor in 1 M HCl solutions. EIS measurement results indicated that the resistance of the carbon steel electrode increased greatly and its capacitance decreases by increasing the inhibitor concentration. The inhibition is accomplished by adsorption of this compound on the iron surface, and the adsorption is spontaneous and obeys the Langmuir isotherm. The inhibiting efficiencies obtained by polarization, EIS and weight loss measurements are in good agreement.

References

1. Solmaz R., Kardaş G., Yazici B., Erbil M. *Colloids Surf. A.* 7 (2008**)** 312.
2. Prajila M., Sam J., Bincy J., Abraham J. *J. Mater. Environ. Sci.* 3 (2012) 1045.
3. Naik U J.,. Panchal V A., Patel A S., Shah N.K., *J. Mater. Environ. Sci.* 3 (2012) 935.
4. Zarrouk A., Zarrok H., Salghi R., Hammouti B., Bentiss F., Touir R., Bouachrine M. *J. Mater. Environ. Sci.* 4 (2013) 177.
5. Zarrok H., Oudda H., Zarrouk A., Salghi R., Hammouti B., Bouachrine M. *Der Pharm. Chem*. 3 (2011) 576.
6. Zarrok H., Salghi R., Zarrouk A., Hammouti B., Oudda H., Bazzi Lh., Bammou L., Al-Deyab S. S. *Der Pharm. Chem*. 4 (2012) 407.
7. Zarrok H., Al-Deyab S. S., Zarrouk A., Salghi R., Hammouti B., Oudda H., Bouachrine M., Bentiss F. *Int. J. Electrochem. Sci*. 7 (2012) 4047.
8. Ben Hmamou D., Salghi R., Zarrouk A., Zarrok H., Hammouti B., Al-Deyab S. S., Bouachrine M., Chakir A., Zougagh M. *Int. J. Electrochem. Sci*. 7 (2012) 5716.
9. Zarrouk A., Hammouti B., Al-Deyab S.S., Salghi R., Zarrok H., Jama C., Bentiss F. *Int. J. Electrochem. Sci*. 7 (2012) 5997.
10. Zarrouk A., Messali M., Zarrok H., Salghi R., Al-Sheikh Ali A., Hammouti B., Al-Deyab S. S., Bentiss F. *Int. J. Electrochem. Sci*. 7 (2012) 6998.
11. Zarrok H., Zarrouk A., Salghi R., Ramli Y., Hammouti B., Al-Deyab S. S., Essassi E. M., Oudda H. *Int. J. Electrochem. Sci*. 7 (2012) 8958.
12. Ben Hmamou D., Salghi R., Zarrouk A., Zarrok H., Al-Deyab S. S., Benali O., Hammouti B. *Int. J. Electrochem. Sci.* 7 (2012) 8988.
13. Zarrouk A., Messali M., Aouad M. R., Assouag M., Zarrok H., Salghi R., Hammouti B., Chetouani A. *J. Chem. Pharm. Res*. 4 (2012) 3427.
14. Ben Hmamou D., Aouad M. R., Salghi R., Zarrouk A., Assouag M., Benali O., Messali M., Zarrok H., Hammouti B. *J. Chem. Pharm. Res*. 4 (2012) 3489.
15. Zarrok H., Oudda H., El Midaoui A., Zarrouk A., Hammouti B., Ebn Touhami M., Attayibat A., Radi S., Touzani R. *Res. Chem. Intermed.* (2012) DOI 10.1007/s11164-012-0525-x
16. Zarrouk A., Hammouti B., Zarrok H., Salghi R., Dafali A., Bazzi Lh., Bammou L., Al-Deyab S S. *Der Pharm. Chem*. 4 (2012) 337.
17. Zarrok H., Zarrouk A., Hammouti B., Salghi R., Jama C., Bentiss F. *Corros. Sci*. 64 (2012) 243.
18. Refaey S A M. *Appl. Surf. Sci*. 240 (2005) 396.
19. Majjane A., Rair D., Chahine A., Et-tabirou M., Ebn Touhami M., Touir R. *Corros. Sci*. 60 (2012) 98.
20. Ashassi-Sorkhabi H., Asghari E. *Corros. Sci*. 51 (2009) 1828.
21. Guannan Mu., Xianghong Li., Qing Qu., Jun Zhou. *Corros. Sci*. 48 (2006) 445.
22. Abdel-Gaber A M., Masoud M S, Khalil E A., Shehata E. E. *Corros. Sci.* 51 (2009) 3021.
23. Bayol E., Kayakirilmaz K., Erbil M. *Mater. Chem. Phys.* 104 (2007) 74.
24. Tang L., Mu G., Liu G. *Corros. Sci*. 45 (2003) 2251.
25. Ferreira E S., Giancomlli C., Giacomlli F C., Spinelli A. *Mater. Chem. Phys*. 83 (2004) 129.
26. Vračar L j M., Dražić D. M. *Corros. Sci*. 44 (2002) 1669.

ISSN : 2528-2028
CODEN: JMESCN

27. Li X H., Deng S D. *Corros. Sci*. 509 (2008) 420.
28. Obot I B., Obi-Egbedi N O. *Corros. Sci*. 52 (2010) 198.
29. Deng S., Li X., Fu H. *Corros. Sci*. 52 (2010) 3840.
30. Issaadi S., Douadi T., Zouaoui A., Chafaa S., Khan M A., Bouet G. *Corros. Sci*. 53 (2011) 1484.
31. Achary G., Sachin H. P., Arthoba Naik Y., Venkatesha T V. *Mater. Chem. Phys*. 107 (2008) 44.
32. Hashim N Z N., Kassim K., Mohd Y. *APCBEE Procedia*. 3 (2012) 239.
33. Vakili Azghandi M., Davoodi A., Farzi G A., Kosari A. *Corros. Sci*. 64 (2012) 44.
34. Hosseini M., Merens S F L, Ghorbani M. *Mater. Chem. Phys*. 78(2003) 800.
35. Benabdellah M., Tounsi A., Khaled K F., Hammouti B. *Arab. J. Chem*. 4 (2011) 17.
36. El-Awady A A., Abd-El-Nabey B A., Aziz S G. J. Electrochem. Soc. 139 (1992) 2149.
37. J.O'M. Bockris, A.K.N. Reddy, Modern Electrochemistry, vol. 2, Plenum Publishing Corporation, New York, (1976).
38. Wang X., Yang H., Wang F. *Corros. Sci*. 52 (2010) 1268.
39. Ebenso E E., Obot I B., Murulana L C. *Int. J. Electrochem. Sci*. 5 (2010) 1574.
40. Migahed M.A. *Mater. Chem. Phys*. 93 (2005) 48.
41. X. Wang, H. Yang, F. Wang. *Corros. Sci.* 53 (2011) 113..
42. Cano E., Polo J. L., La Iglesia A., Bastidas J M. *Adsorption*. 10 (2004) 219.
43. Bentiss F., Lebrini M., Lagrenée M. *Corros. Sci. 47* (2005) 2915.
44. Li X., Deng S., Fu H., *Corros. Sci*. 53 (2011) 302.
45. Hosseini S M A., Salari M., Ghasemi M., Abaszadeh M. *Z. Phys. Chem*. 223 (2009) 769.
46. Ghareba S., Omanovic S. *Corros. Sci.* 52 (2010) 2104.
47. Mert B D., Mert M E, Kardas G., Yazici B. *Corros. Sci*. 53 (2011) 4265.
48. Noor E A., Al-Moubaraki A H. *Mater. Chem. Phys*. 110 (2008) 145.
49. Solmaz R., Kardas G., Çulha M., Yazici B., Erbil M. *Electrochim. Acta*. 53 (2008) 5941.
50. Beck F., Kruger U.A. *Electrochim. Acta*, 41 (1996) 1083.
51. Sanchez-Tovar R., Montanes M.T., Garcia-Anton J. *Corros. Sci.* 52 (2010) 722.
52. Martinez S., Stern I. *Appl. Surf. Sci.* 199 (2002) 83.
53. Khadom A.A., Yaro A.S., Kadhum A.A.H., Al Taie A.S., Musa A.Y., *Amer. J. Appl. Sci.*, 6 (2009) 1403.
54. Guan N M., Xueming L., Fei L. *Mater. Chem. Phys.* 86 (2004) 59.
55. Zarrok H., Al Mamari K., Zarrouk A., Salghi R., Hammouti B., Al-Deyab S S., Essassi E M., Bentiss F., Oudda H. *Int. J. Electrochem. Sci.* 7 (2012) 10338 .